RSC Advances

COMMUNICATION

View Article Online
View Journal | View Issue

Cite this: *RSC Adv.*, 2014, **4**, 39572

Received 3rd June 2014
Accepted 8th August 2014

DOI: 10.1039/c4ra05268d

www.rsc.org/advances

Highly efficient reversible adsorption of NO_2 in imidazole sulfonate room temperature ionic liquids†

Gang Yuan, Feng Zhang, Jiao Geng* and You-Ting Wu*

The highly efficient reversible adsorption of NO_2 in room-temperature ionic liquids is reported for the first time, making a platform for promising applications.

Controllable dissolution of nitrogen oxides (NO_x) is of great importance for the design and application of hypergolic fuel, organic synthesis (such as oxidation, nitration and nitrosation),[1–4] and NO_x sensing.[5] As a main source of air pollution, NO_x contains huge amount of wasted energy which is difficult to reuse.[6] Though species as NO_2 and N_2O_4 have been theoretically proved to be ideal oxidizer,[7] it is problematic in handling and application,[2,8] unless they are easily stored and reacted as our wishes. Here, imidazole sulfonate ionic liquids (ILs) were found to be ideal solvent for NO_2, and, what's more, the adsorption of NO_2 in such ILs was reversible upon simple operations. The study of such reversible adsorption process provides not only a highly efficient method to separate NO_2, but also a promising and fascinating way to utilize the wasted energy in NO_x.

With the advantages of ideal interfacial properties, negligible vapor pressure, thermal stability, favorable viscosity, miscibility with water and organic solvents, good abilities to extract metal ions and compounds, and environmentally friendly,[9–13] ILs have been used in fields such as separation, bioanalytical preconcentration and detection, organic synthesis, and catalysis.[14–19] Therefore, there has been an explosion of interest in the research of ionic liquids in recent years.[13] The capture or sensing of gasses as N_2, CO_2, SO_2, and NO_2 in ILs has been studied,[5,20–24] however, to the best of our knowledge, the reversible adsorption of NO_2 and the interaction between cations and NO_2 or N_2O_4 molecule in ILs have not been reported yet, although such process is of huge application potential in the fields as synthesis and energy utilization.

In our study, the imidazole sulfonate room-temperature ILs including 1-ethyl-3-methylimidazolium trifluoromethanesulfonate ([Emim]OTf), 1-butyl-3-methylimidazolium trifluoromethanesulfonate ([Bmim]OTf), and 1-hexyl-3-methylimidazolium trifluoromethanesulfonate ([HMIM]O-TF) were chosen to be the solvent. The reversible adsorptions of NO_2 in these room-temperature ILs were found, respectively. In addition, N_2O_4 was produced after the adsorption in each IL.

As shown in Fig. 1, for [Hmim]OTf, the color of the solution turned cyan blue after the adsorption of NO_2 at the pressure of 40 kPa and the temperature of 35 °C (Fig. 1, insert left). Compared with the UV-vis adsorption spectrum of [Hmim]OTf (Fig. 1, blue line), six hyperfine split peaks at the wavelengths of 324.6 nm, 335.3 nm, 346.0 nm, 358.8 nm, 372.2 nm, and

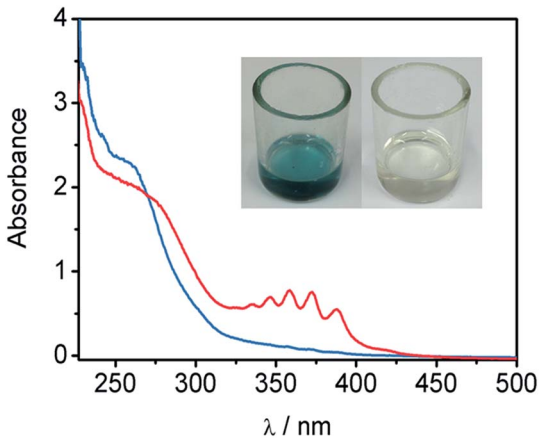

Fig. 1 UV-vis spectra of [Hmim]OTf before (blue line) and after (red line) adsorption of NO_2. Insert: the photograph of [Hmim]OTf with NO_2 in it (left) and after release of NO_2 (right). The adsorption pressure was 40 kPa.

Department of Chemical Engineering, School of Chemistry and Chemical Engineering, Nanjing University, Nanjing 210093, P. R. China. E-mail: gengjiao@nju.edu.cn; ytwu@nju.edu.cn; Fax: +86 25 83595559; Tel: +86 25 83595559

† Electronic supplementary information (ESI) available: Materials, methods, the UV-vis spectra of [Emim]OTf and [Hmim]OTf before and after adsorption of NO_2, the FTIR spectra of ILs before and after adsorption of NO_2, the amount of the pressure changes during the adsorption at different initial pressures, and the pressure changes upon the adsorption of NO_2 in the ILs at different temperatures. See DOI: 10.1039/c4ra05268d

387.9 nm, respectively, appeared after the adsorption (Fig. 1, red line), resulting from the vibrational electronic transition of N_2O_4.[25–28] The same color change appeared with [Emim]OTf and [Bmim]OTf after adsorbing NO_2 at the same condition.

However, different from [Hmim]OTf and [Bmim]OTf, a new peak at 417.0 nm appeared on the spectrum of [Emim]OTf after adsorbing NO_2 as well as the six fine peaks (Fig. 1 and S1 in ESI†), which should be ascribed to the UV-vis adsorption of NO_2 monomer.[26–28] The great tendency of NO_2 monomer to become the dimer led to the formation of N_2O_4. Meanwhile, the structure of π bond of N_2O_4 is prone to form π_{cation}–π interaction with imidazole cation in the ILs,[29] which could be a main factor contributed to the adsorption state of NO_2 in these ILs. The cyan blue color was probably due to the π_{cation}–π interaction and the ion interaction induced charge transfer. The disintegration of N_2O_4 was easier among the molecules of [Emim]OTf than in the other two ILs, since the smaller steric hindrance of alkyl on [Emim]OTf made room for the stronger molecular motion of N_2O_4. Therefore, the ratio of NO_2 monomer was bigger in [Emim]OTf than in [Bmim]OTf and [Hmim]OTf, leading to the obvious additional adsorption peak at the wavelength of 417.0 nm (Fig. S1a in ESI†). This fact also referred that the six split peaks around 320–390 nm attributed most to N_2O_4.

The Fourier transform infrared (FTIR) spectra of [Emim]OTf, [Bmim]OTf, and [Hmim]OTf were recorded before and after the adsorption of NO_2, respectively (Fig. S2 in ESI†). After the adsorption of NO_2, a new transmission peak at 1665 cm^{-1} was recorded with [Emim]OTf and [Bmim]OTf, respectively (Fig. S2a and S2b in ESI†). Meanwhile, for [Hmim]OTf the new peak appeared at 1662 cm^{-1}. These peaks should be ascribed to the a-stretch vibration of N_2O_4.[30] The slight red-shift of IR adsorption in [Hmim]OTf was probably because that the inductive effect and the steric hindrance of –hexyl constrained the a-stretch vibration, leading to the vibration strength. While the same effect of –ethyl and –butyl were not as strong as –hexyl. Accompany with the UV-vis spectra, the FTIR spectra (Fig. S2 in ESI†) confirmed the existence of N_2O_4, indicating the successful adsorption and stabilization of NO_2 by the imidazole sulfonate ILs.

With the help of π_{cation}–π interaction between N_2O_4 and the imidazole sulfonate IL molecules, the adsorbed N_2O_4 could remain stable in these ILs in the closed container. After 2 months, the colors of the solutions still remained unchanged. Once open to the air at 25 °C, NO_2 will gradually release from the solvent. The color of the solution turned from dark cyan blue to yellow and to transparent eventually. The time of release depends on the solvent. Generally, in [Emim]OTf, it spent about 2 hours, in [Bmim]OTf it was 5 hours, and 20 hours for [Hmim]OTf, indicating reversible adsorption–desorption properties.

To investigate the reversible adsorption–desorption process, vacuum conditions were applied so that the N_2O_4 and NO_2 dissolved in the ILs could release immediately. Two containers (one for gas storage and the other for adsorption) were connected together with a valve. A vacuum pump and a pressure sensor were also connected to the system so that the gas pressure could be controlled. At the initial pressure of NO_2 as 40 kPa, the adsorption processes were conducted in 4 g [Emim]-OTf, [Bmim]OTf, and [Hmim]OTf, respectively. With the help of vacuum-assisted desorption, pressure changes during 4 cycles of adsorption–desorption processes in each IL were recorded as shown in Fig. 2. The pressures of the connected system, which was positively related to the remained amount of NO_2, decreased rapidly indicating the fast adsorption of NO_2 in these ILs. The adsorption equilibrium achieved after about 100 s in [Emim]OTf and [Bmim]OTf (Fig. 2a and b), respectively, and 280 s in [Hmim]OTf (Fig. 2c). The longer adsorption time in [Hmim]-OTf probably resulted from the bigger steric hindrance of –hexyl on Hmim molecule than –ethyl on Emim and –butyl on Bmim (Fig. 2, insert), which made it more difficult for NO_2 to enter the space among [Hmim]OTf molecules and located on the best adsorption site.

During the second adsorption round, the equilibrium achieved later compared with the first one in all the ILs. It spent about 130 s in [Emim]OTf (Fig. 2a), 175 s in [Bmim]OTf (Fig. 2b), and 450 s in [Hmim]OTf (Fig. 2c), respectively. Meanwhile, more NO_2 was adsorbed in each IL, which was probably because the adsorbed NO_2 in the first adsorption–desorption process made path and room in IL molecules for the followed NO_2 molecules, just like what happens in molecular imprinting. The more amount of NO_2 adsorption led to the longer adsorption time in each IL. As shown in Fig. 2, the molecular-imprinting like processes achieved their equilibriums at 360 s in [Emim]OTf (the second adsorption–desorption round), 630 s in [Bmim]OTf (the third round), and 900 s in [Hmim]OTf (the second round), respectively, showing that the bigger the steric hindrance of alkyl group on the imidazole cation, the longer the imprinting time was. This fact, together with the FTIR results, indicates

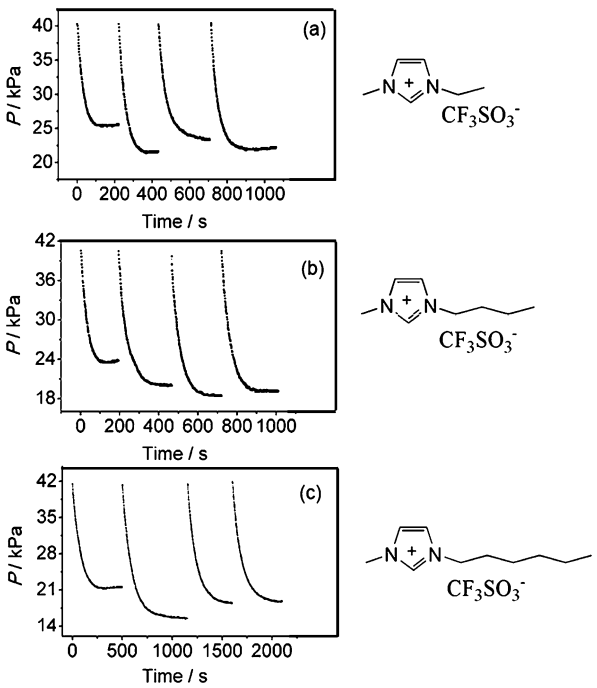

Fig. 2 The pressure change upon the adsorption–desorption cycles of NO_2 in [Emim]OTf (a), [Bmim]OTf (b), and [Hmim]OTf (c) at 35 °C. Insert is the structural formula of each IL.

that the adsorption of NO_2 (taking form of dimer) was through the interaction with the imidazole parts of ILs. After the imprinting process, some of NO_2 molecules were deeply adsorbed by the ILs and could not be driven out by simply applying vacuum condition, so that they could not be replaced by the NO_2 molecules in the next round. Therefore, the adsorption amount of NO_2 decreased in the next adsorption round, but still more than the first round without the molecular-imprinting like process.

Both of the pressure changes in the adsorption–desorption processes and the molecular-imprinting like processes illustrate that the adsorption of NO_2 in the imidazole sulfonate ILs is reversible and controllable, unlike in water and the other solvents. The solubility of NO_2 in each IL was evaluated at different initial pressures. There is the linear relationship between the dissolved amount of NO_2 in unit gram of IL (C_{NO_2}, calculated from the pressure change shown in Fig. S3 in ESI†) and the initial pressure (P_0), which is $P_0 = 0.46\ C_{NO_2} - 2.28$ ($R^2 = 0.95$) in [Emim]OTf; $P_0 = 0.61\ C_{NO_2} - 4.05$ ($R^2 = 0.99$) in [Bmim]OTf; and $P_0 = 0.67\ C_{NO_2} - 5.00$ ($R^2 = 0.98$) in [Emim]OTf, respectively (Fig. 3). The good but simple linear ship is in accordance with Henry's Law, indicating the inexistence of complex chemical reactions the solute and the solvent during the adsorption. Additionally, the average amount of NO_2 adsorbed in these three ILs at 60 kPa was 32.2 mg g^{-1}, which means 15.7 mL NO_2 at the standard state could be adsorbed into 1 g solvent.

Besides, the reversible adsorption of NO_2 in the ILs was studied with the temperature changing from 35 °C to 65 °C. With the initial pressure of 42 kPa, the solubility of NO_2 in the ILs decreased as the temperature grew up (Fig. S4 in ESI†). The equilibrium pressure at 45 °C, 55 °C, and 65 °C were almost the same in [Emim]OTf (Fig. S4a in ESI†), but different from each other in [Bmim]OTf and [Hmim]OTf, especially in the latter (Fig. S4b and S4c†). Moreover, the equilibrium pressures at 65 °C in the three ILs were almost the same (Fig. S4 in ESI,† 29.3 kPa for [Emim]OTf, 31.4 kPa for [Bmim]OTf, and 30.9 kPa for [Hmim]OTf). The different variation rate of the equilibrium pressures towards the temperature in the different ILs is proposed to be resulted from the different molecular motion of N_2O_4 in each IL. In [Emim]OTf, the steric hindrance is smaller than the other two solvents, leading to the smaller intermolecular fraction. Therefore, the frequency and strength of the motion of N_2O_4 molecules in [Emim]OTf increased rapidly as the temperature grew up, which is in accordance with the UV-vis spectrum (Fig. S1 in ESI,† the extra peak appeared at 417.0 nm). As a result, the internal energy of the N_2O_4-[Emim]OTf increased rapidly, which means the adsorption enthalpy change (ΔH) increased rapidly with the temperature growth. Thus the adsorption equivalent shifted to the left rapidly, leading to the rapid equilibrium-pressure growth with the temperature growth. On the other hand, in [Hmim]OTf the bigger hindrance led to the slower changing rate of the reaction enthalpy, so that the equilibrium pressure grew slower. As the temperature grew, the increase of the frequency and strength of N_2O_4 molecular motion gradually slowed down, since the bigger constraint resulting from the molecular body of each IL. Therefore the motion in different IL eventually tended to be almost the same level, leading to nearly the same equilibrium pressures in three ILs at 65 °C. In addition, NO_2 exists in equilibrium with the colourless N_2O_4 as an exothermic process with enthalpy change of about −57 kJ mol^{-1}.[31,32] NO_2 will be favoured at high temperatures. This single equilibrium existed in all of the three ILs, thus did not interfere with the change of equilibrium pressures. The temperature related adsorption proves the proposed adsorbing mechanism again and provides important data for the application in the scenes of real work.

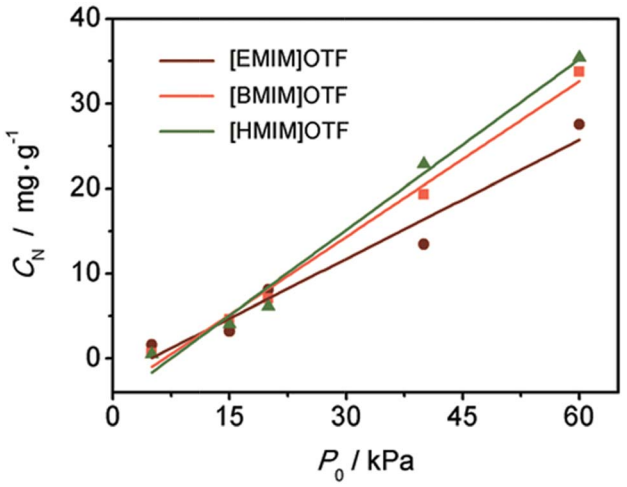

Fig. 3 The relationship between the amount of NO_2 adsorbed in unit gram of IL (C_{NO_2}), in different ILs (left corner), and the initial pressure (P_0).

To sum up, NO_2 can be reversibly adsorbed in imidazole sulfonate room temperature ILs and takes form of dimer among IL molecules. Unlike in water and the other solvents, the molecular-imprinting like process was found during the adsorption–desorption cycles in these ILs. The solubility of NO_2 in different ILs depends on the initial pressure, temperature, and the steric hindrance of alkyl on imidazole cation. The well adsorbed NO_2 can be conveniently used in the fields like fuel cell design and the possible organic synthesis, which opens a new way to separate and utilize the wasted energy in nitrogen oxides. We believe these initial results will make our life cleaner and the energy be utilized more efficiently in varieties of chemical industries.

Acknowledgements

This work was financially supported by the Project of Jiangsu province research prospective study (BY2013072-07).

Notes and references

1 W. G. Liu and W. A. Goddard, *J. Am. Chem. Soc.*, 2012, **134**, 12970–12978.
2 C. Nonnenberg, I. Frank and T. M. Klapotke, *Angew. Chem., Int. Ed.*, 2004, **43**, 4585–4589.
3 R. A. Pierce, R. P. Campbell-Kelly, A. E. Visser and J. E. Laurinat, *Ind. Eng. Chem. Res.*, 2007, **46**, 2372–2376.

4 A. Commeyras, H. Collet, L. Boiteau, J. Tailades, O. Vandenabeele-Trambouze, H. Cottet, J. P. Biron, R. Plasson, L. Mion, O. Lagrille, H. Martin, F. Selsis and M. Dobrijevic, *Polym. Int.*, 2002, **51**, 661–665.
5 R. Toniolo, N. Dossi, A. Pizzariello, A. P. Doherty and G. Bontempelli, *Electroanalysis*, 2012, **24**, 865–871.
6 L. N. Lamsal, R. V. Martin, D. D. Parrish and N. A. Krotkov, *Environ. Sci. Technol.*, 2013, **47**, 7855–7861.
7 Y. Liu, S. V. Zybin, J. Guo, A. C. T. van Duin and W. A. Goddard, *J. Phys. Chem. B*, 2012, **116**, 14136–14145.
8 P. Rumbach, M. Witzke, R. M. Sankaran and D. B. Go, *J. Am. Chem. Soc.*, 2013, **135**, 16264–16267.
9 L. B. Escudero, A. C. Grijalba, E. M. Martinis and R. G. Wuiloud, *Anal. Bioanal. Chem.*, 2013, **405**, 7597–7613.
10 L. B. Escudero, P. Berton, E. M. Martinis, R. A. Olsina and R. G. Wuiloud, *Talanta*, 2012, **88**, 277–283.
11 C. H. Xu, A. Durumeric, H. K. Kashyap, J. Kohanoff and C. Margulis, *J. Am. Chem. Soc.*, 2013, **135**, 17528–17536.
12 T. Welton, *Chem. Rev.*, 1999, **99**, 2071–2084.
13 K. R. J. Lovelock, I. J. Villar-Garcia, F. Maier, H. P. Steinrück and P. Licence, *Chem. Rev.*, 2010, **110**, 5158–5190.
14 T. Welton and J. P. Hallett, *Chem. Rev.*, 2011, **111**, 3508–3576.
15 D. S. Silvester, *Analyst*, 2011, **136**, 4871–4882.
16 W. Qian, E. Jin, W. Bao and Y. Zhang, *Angew. Chem., Int. Ed.*, 2005, **44**, 952.
17 D. B. G. Williams, M. Ajam and A. Ranwell, *Organometallics*, 2007, **26**, 4692.
18 N. V. Plechkova and K. R. Seddon, *Chem. Soc. Rev.*, 2008, **37**, 123.
19 C. F. Poole and S. K. Poole, *J. Chromatogr. A*, 2010, **1217**, 2268–2286.
20 X. H. Huang, C. J. Margulis, Y. H. Li and B. J. Berne, *J. Am. Chem. Soc.*, 2005, **127**, 17842–17851.
21 C. Wang, G. Cui, X. Luo, Y. Xu, H. Li and S. Dai, *J. Am. Chem. Soc.*, 2011, **133**, 11916–11919.
22 S. M. Mahurin, T. Dai, J. S. Yeary, H. Luo and S. Dai, *Ind. Eng. Chem. Res.*, 2011, **50**, 14061–14069.
23 S. Ren, Y. Hou, W. Wu and M. Jin, *Ind. Eng. Chem. Res.*, 2011, **50**, 998–1002.
24 L. L. Zhang, J. X. Wang, Y. Xiang, X. F. Zeng and J. F. Chen, *Ind. Eng. Chem. Res.*, 2011, **50**, 6957–6964.
25 M. F. Merienne, A. Jenouvrier, B. Coquart and J. P. Lux, *J. Atmos. Chem.*, 1997, **27**, 219–232.
26 K. Yoshino, J. R. Esmond and W. H. Parkinson, *Chem. Phys.*, 1997, **221**, 169–174.
27 J. Orphal, *J. Photochem. Photobiol., A*, 2003, **157**, 185–209.
28 J. N. Crowley and S. A. Carl, *J. Phys. Chem. A*, 1997, **101**, 4178–4184.
29 V. Georgakilas, M. Otyepka, A. B. Bourlinos, V. Chandra, N. Kim, K. C. Kemp, P. Hobza, R. Zboril and K. S. Kim, *Chem. Rev.*, 2012, **112**, 6156–6214.
30 H. Beckers, X. Zeng and H. Willner, *Chem.–Eur. J.*, 2010, **16**, 1506–1520.
31 C. S. Sharov, E. A. Konstantinova, L. A. Osminkina, V. Y. Timoshenko and P. K. Kashkarov, *J. Phys. Chem. B*, 2005, **109**, 4684–4693.
32 J. Barin and O. Knacke, *Thermochemical Properties of Inorganic Sunstances*; Springer, Berlin, 1977.